Performance Evaluation of MIMO-OFDM/OQAM in Time-varying Underwater Acoustic Channels

Mohammud J. Bocus, Angela Doufexi, and Dimitris Agrafiotis
Department of Electrical and Electronic Engineering, University of Bristol, BS8 1UB, UK.

***Abstract*— In this paper we evaluate the bit error rate (BER) performance of coded and un-coded spatially-multiplexed multiple-input multiple-output (MIMO) filter bank multi-carrier (FBMC) and Orthogonal Frequency Division Multiplexing (OFDM) systems for both horizontally and vertically configured time-varying underwater acoustic channels (UACs). OFDM/Offset Quadrature Amplitude Modulation (OFDM/OQAM) is selected as the FBMC system since it achieves maximum bandwidth efficiency. The theoretical achievable bit rates of the MIMO systems are also presented for both channel configurations. Preamble-based channel estimation using the Interference Approximation Method (IAM) is considered. We show that the MIMO-OFDM/OQAM systems achieve a better error performance and also a higher bit rate than the MIMO-OFDM systems in both the horizontal and vertical channels. This makes FBMC very attractive for wirelessly transmitting multimedia data such as real-time video in an UAC where the bandwidth is extremely limited.**

I. Introduction

The underwater acoustic channel (UAC) is often regarded as one of the most challenging medium in use today since it combines the worst properties of a mobile terrestrial radio channel in terms of poor physical link quality and high latency of a satellite link [1]. Applications which involve real time video transmission can be a serious challenge in an UAC due to the very limited acoustic bandwidth. High quality videos usually have large information content and hence require a high bit rate. In this regard OFDM has been widely investigated for underwater acoustic (UWA) communication mainly due to its robustness against intersymbol interference (ISI) by using a cyclic prefix (CP), high bandwidth efficiency and simple frequency domain equalization. While the CP is a fundamental part of OFDM, its usage represents a wastage of useful bits which could have been otherwise used for transmitting data. The delay spread in an UAC can span over tens or even hundreds of milliseconds and therefore the OFDM symbol duration is often very long. Hence, there may be too much channel variation across the OFDM symbols and any slight motion between the transmitter and receiver can result in inter-carrier interference (ICI).

FBMC systems in contrast do not require any CP to achieve robust performance in doubly-dispersive channels. This can be achieved using prototype filters which exhibit good time/frequency localization (TFL) such as Isotropic Orthogonal Transform Algorithm (IOTA) [2] and Hermite filters [3]. Only a few studies have investigated FBMC systems for UWA communication. A Filtered Multitone (FMT) system was used in [4] with 32 wideband subcarriers for a link distance of 800 m and water depth of 100 m. The system bandwidth was varied between 1.5 to 4.5 kHz and the maximum achievable bit rate was 6 $kbps$. Simulation results showed that when there is channel variation, FMT may provide a better performance than OFDM. In order to cope with doubly-dispersive UACs, the authors of [5] proposed a prototype filter for a FMT system with hexagonal lattice structure based on the Hermite functions. In this FMT system, the subcarriers slightly overlapped. By considering the signal-to-interference ratio (SIR), the modified FMT system provided a better performance than both the conventional FMT and OFDM systems. In [6], a Doppler compensation algorithm was proposed for a Cosine Multitone (CMT) system with 64 subcarriers. The low complexity algorithm is based on frequency spreading. Simulations results showed that when a Doppler scaling factor ξ was varied from 0 to 0.05, the SIR of the CMT system had a fairly constant value of 65 dB.

While MIMO-OFDM has been widely investigated for UWA communication (e.g [7], [8]), to the best of the authors' knowledge MIMO-OFDM/OQAM has not been considered for the UWA scenario. In this paper, we examine the BER performance comparison between MIMO-OFDM and MIMO-OFDM/OQAM in two time-varying channel configurations; vertical and horizontal. Preamble-based channel estimation using the Interference Approximation Method (IAM) is applied to both the MIMO-OFDM and MIMO-OFDM/OQAM systems. We also use Turbo coding since the UAC is susceptible to a large number of bit errors. Finally we provide the theoretical achievable bit rates with both systems for the two channel scenarios.

The rest of the paper is organized as follows: Section II provides the discrete-time baseband model for a SISO and MIMO-OFDM/OQAM system. Section III describes the typical characteristics of an UAC. Section IV presents simulation results of the systems in horizontally and vertically configured UACs. Conclusions are given at the end of this paper.

$Notation$. Matrices and vectors are denoted by bold uppercase and lowercase letters respectively. The complex conjugate of a letter x is given as $x^{\star}$. The superscript ^{T} denotes a transpose operation.

II. System Model

A. SISO-OFDM/OQAM

In OFDM/OQAM real symbols are transmitted at twice the rate of OFDM/QAM, allowing prototype filters with good

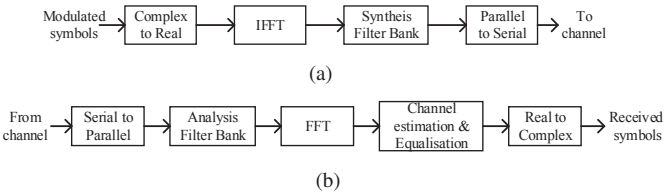

Fig. 1. Basic OFDM/OQAM block diagram. (a) Transmitter (b) Receiver

TFL property to be used, while still ensuring maximum bandwidth efficiency. However in OFDM/OQAM orthogonality only holds in the real field and therefore there will always be some kind of intrinsic imaginary interference between neighboring subcarriers and symbols that makes channel estimation difficult [9]. OFDM/OQAM is analogous to CP-OFDM, the only difference being the introduction of filter banks at the transmitter and receiver and removal of CP block. The basic block diagram of OFDM/OQAM transceiver system is shown in Fig. 1. The discrete-time signal at the synthesis filter bank (SFB) output is represented as [9]

$$s(l) = \sum_{m=0}^{M-1} \sum_{n} d_{m,n} g_{m,n}(l), \tag{1}$$

where $d_{m,n}$ are the real OQAM symbols and

$$g_{m,n}(l) = g(l - n\frac{M}{2}) e^{j\frac{2\pi}{M} m (l - \frac{L_g - 1}{2})} e^{j\phi_{m,n}}, \tag{2}$$

with g representing the real symmetric prototype filter impulse response of length L_g, M is the number of subcarriers and $\phi_{m,n} = \phi_0 + \frac{\pi}{2}(m+n) mod\ \pi$ and ϕ_0 can be chosen to have an arbitrary value [9]. The notations m and n represent the subcarrier and OQAM symbol time indices respectively. Without loss of generality we define $\phi_{m,n}$ as $(m+n)\frac{\pi}{2} - mn\pi$ as in [9]. The filter length is $L_g = KM$ with K being the filter overlapping factor. The prototype filter g is designed such that the subcarrier functions $g_{m,n}$ are orthogonal in the real field [9]. So if we consider an ideal channel with no distortion and noise and assuming perfect time/frequency synchronization, there will be intrinsic interference at the output of the analysis filter bank (AFB) which can be denoted as [9]

$$\sum_{l} g_{m,n}(l) g^{\star}_{p,q}(l) = \jmath \langle g \rangle^{p,q}_{m,n}, \tag{3}$$

where $\langle g \rangle^{p,q}_{m,n} = -\jmath \langle g_{m,n} | g_{p,q} \rangle$ and $\langle g_{m,n} | g_{p,q} \rangle$ represents a purely imaginary term for $(m,n) \neq (p,q)$ [10]. Assuming that each subcarrier experiences flat fading and that the channel is constant over the duration of the prototype filter which is true for practical values of channel length L_h and L_g and for prototype filters g's which are well localized in time, one can define the output of the AFB at the pth subcarrier and qth OFDM/OQAM symbol as [9]

$$y_{p,q} = H_{p,q} d_{p,q} + \underbrace{\jmath \underbrace{\sum_{m=0}^{M-1} \sum_{n}}_{(m,n) \neq (p,q)} H_{m,n} d_{m,n} \langle g \rangle^{p,q}_{m,n}}_{I_{p,q}} + \eta_{p,q}, \tag{4}$$

where $H_{p,q}$ is the M-point channel frequency response (CFR), $I_{p,q}$ and $\eta_{p,q}$ are the interference and noise components respectively. Provided a prototype filter with good TFL property is used, one can assume that the intrinsic imaginary interference only comes from the first-order neighborhood of (p,q) such that $\Omega_{p,q} = \{(p \pm 1, q \pm 1), (p, q \pm 1), (p \pm 1, q)\}$. Furthermore assuming an almost constant CFR over this neighborhood, (4) can be approximated as [9]

$$y_{p,q} \approx H_{p,q} c_{p,q} + \eta_{p,q}, \tag{5}$$

where

$$c_{p,q} = d_{p,q} + \jmath \underbrace{\sum_{(m,n) \in \Omega_{p,q}} d_{m,n} \langle g \rangle^{p,q}_{m,n}}_{u_{p,q}} = d_{p,q} + \jmath u_{p,q}, \tag{6}$$

is the virtual transmitted symbol at (p,q) and

$$u_{p,q} = \sum_{(m,n) \in \Omega_{p,q}} d_{m,n} \langle g \rangle^{p,q}_{m,n}, \tag{7}$$

is the imaginary part of the interference from the neighboring frequency-time (FT) points. The CFR estimate at a given FT point can be obtained as follows [9]

$$\hat{H}_{p,q} = \frac{y_{p,q}}{c_{p,q}} \approx H_{p,q} + \frac{\eta_{p,q}}{c_{p,q}}. \tag{8}$$

The preambles are designed such that the pseudo-pilots have maximum magnitude. Thus the training symbols surrounding the pilot $d_{p,q}$ should allow all the terms in (7) to have similar sign in order for them to add together for all frequencies p [9]. In this respect the interference weights $\langle g \rangle^{p,q}_{m,n}$ need to be computed for neighbors $(m,n) \in \Omega_{p,q}$ at each FT point (p,q). For all symbols q, the weights follow the pattern [9]

$$\begin{array}{ccc} (-1)^p\delta & -\beta & (-1)^p\delta \\ -(-1)^p\gamma & d_{p,q} & (-1)^p\gamma \\ (-1)^p\delta & \beta & (-1)^p\delta \end{array} \tag{9}$$

where the horizontal and vertical directions correspond to time and frequency respectively. β, γ, δ are positive with values less than 1 and generally β and γ are greater than δ.

A few IAM preamble variants have been proposed in literature; namely IAM-R [10], IAM-I [11] and IAM-C [12]. The latter is a complex-based preamble and is considered in this work. In [12] it was shown that the IAM-C preamble structure provides good performance in channels characterized by both delay and Doppler spreads. Also, the IAM-C preamble slightly outperforms the IAM-R and IAM-I preambles. The three preamble structures are shown in Fig. 2 for the single-input single-output (SISO) case where $M = 8$ and OQPSK modulation is assumed. The preamble duration for the SISO system spans over three FBMC/OQAM symbols, i.e., 1.5 complex OFDM/QAM symbols. As we observe in Fig. 2, the pilot vector lies between two zero vectors. This is required to prevent the pilot vector from being affected by interference from the data symbols (from both the previous and current frames).

0	1	0	0	d_0	0	0	1	0
0	-1	0	0	$-jd_0$	0	0	-j	0
0	-1	0	0	$-d_0$	0	0	-1	0
0	1	0	0	$-d_1$	0	0	j	0
0	1	0	0	jd_1	0	0	1	0
0	-1	0	0	d_1	0	0	-j	0
0	-1	0	0	$-d_0$	0	0	-1	0
0	1	0	0	jd_0	0	0	j	0
(a)			(b)			(c)		

Fig. 2. SISO preambles (a) IAM-R (b) IAM-I (d_0,$d_1 \in \{1, -1\}$) (c) IAM-C

0	1	0	1	0	0	1	0	-1	0
0	-j	0	-j	0	0	-j	0	j	0
0	-1	0	-1	0	0	-1	0	1	0
0	j	0	j	0	0	j	0	-j	0
0	1	0	1	0	0	1	0	-1	0
0	-j	0	-j	0	0	-j	0	j	0
0	-1	0	-1	0	0	-1	0	1	0
0	j	0	j	0	0	j	0	-j	0
(a)					(b)				

Fig. 3. 2 x N_r IAM-C preamble (a) Transmitter 1 (b) Transmitter 2

B. MIMO-OFDM/OQAM

Applying the above formulations to a MIMO system with N_t transmitters and N_r receivers, the signal at each receive antenna can be written as [9]

$$y_{p,q}^{j} = \sum_{i=1}^{N_t} H_{p,q}^{j,i} c_{p,q}^{i} + \eta_{p,q}^{j}, \quad j = 1, 2, \cdots, N_r \tag{10}$$

where $H_{p,q}^{j,i}$ is the M-point CFR form the ith transmit antenna to the jth receive antenna, $c_{p,q}^{i}$ and $\eta_{p,q}^{i}$ are the corresponding virtual symbol and noise component respectively. An overall input-output equation for the MIMO-OFDM/OQAM system can be written as [9]

$$\boldsymbol{y}_{p,q} = \boldsymbol{H}_{p,q}\boldsymbol{c}_{p,q} + \boldsymbol{\eta}_{p,q}, \tag{11}$$

where

$$\boldsymbol{y}_{p,q} = \begin{bmatrix} y_{p,q}^{1} & y_{p,q}^{2} & \cdots & y_{p,q}^{N_r} \end{bmatrix}^T,$$

$$\boldsymbol{\eta}_{p,q} = \begin{bmatrix} \eta_{p,q}^{1} & \eta_{p,q}^{2} & \cdots & \eta_{p,q}^{N_r} \end{bmatrix}^T,$$

$$\boldsymbol{H}_{p,q} = \begin{bmatrix} H_{p,q}^{1,1} & H_{p,q}^{1,2} & \cdots & H_{p,q}^{1,N_t} \\ H_{p,q}^{2,1} & H_{p,q}^{2,2} & \cdots & H_{p,q}^{2,N_t} \\ \vdots & \vdots & \ddots & \vdots \\ H_{p,q}^{N_r,1} & H_{p,q}^{N_r,2} & \cdots & H_{p,q}^{N_r,N_t} \end{bmatrix}.$$

We need at least $2N_t$+1 OFDM/OQAM symbol durations to estimate the CFR [9]. As an example, a $2\times N_r$ MIMO system is considered. The IAM-C preamble structure in this case is shown in Fig. 3 with M=8 and OQPSK modulation assumed. Considering only the pilot vectors at times q=1,3, (11) can be re-written as [9]

$$\begin{bmatrix} \boldsymbol{y}_{p,1} & \boldsymbol{y}_{p,3} \end{bmatrix} = \boldsymbol{H}_{p,1} \begin{bmatrix} c_{p,1}^{1} & c_{p,3}^{1} \\ c_{p,1}^{2} & c_{p,3}^{2} \end{bmatrix} + \begin{bmatrix} \boldsymbol{\eta}_{p,1} & \boldsymbol{\eta}_{p,3} \end{bmatrix}. \tag{12}$$

Analyzing the preamble in Fig. 3, one can notice that $c_{p,1}^{1} = c_{p,3}^{1} = c_{p,1}^{2} = -c_{p,3}^{2} \equiv c_p$. Therefore we can write

$$\begin{bmatrix} \boldsymbol{y}_{p,1} & \boldsymbol{y}_{p,3} \end{bmatrix} = \boldsymbol{H}_{p,1} c_p \boldsymbol{B}_2 + \begin{bmatrix} \boldsymbol{\eta}_{p,1} & \boldsymbol{\eta}_{p,3} \end{bmatrix}, \tag{13}$$

where $\boldsymbol{B}_2$ is a $Hadamard$ matrix of order N_t. The CFR estimate is obtained as follows

$$\hat{\boldsymbol{H}}_{p,1} = \begin{bmatrix} \boldsymbol{y}_{p,1} & \boldsymbol{y}_{p,3} \end{bmatrix} \frac{1}{c_p} \boldsymbol{B}_2^{-1}. \tag{14}$$

In order to design a wireless communication system, a proper understanding of the channel is required. In this regard, the main UAC characteristics which are widely available in literature are described in the following section.

III. Underwater Acoustic Channel

The main factors that characterize the UAC include transmission loss, ambient noise, multipath propagation (causing time spreading), propagation delay and Doppler Effect (causing time variability).

A. Transmission Loss

Transmission loss is both distance (x) and frequency (f) dependent and high frequency acoustic waves are more attenuated than low frequency ones for a given distance. The transmission loss (in dB) is given by [13]

$$10\log A(x, f) = k.10\log x + x.10\log \alpha(f) \tag{15}$$

where $\alpha(f)$ is the absorption coefficient in dB/km, x is the distance in meters, k represents the geometrical spreading factor which takes values between 1 and 2 for shallow and deep water respectively. The Thorp Model can be used to compute $\alpha(f)$ (in dB/km) as follows

$$10\log\alpha(f) = \frac{0.11f^2}{1+f^2} + \frac{44f^2}{4100+f^2} + 2.75\times10^{-4}f^2 + 0.003 \tag{16}$$

The absorption coefficient can alternatively be computed using the Fisher and Simmons model which considers the effects of pressure, salinity, temperature and relaxation frequencies due to boric acid and magnesium sulphate [14].

B. Propagation Delay

The low speed of sound in water ($\approx$1500 m/s) causes a high propagation delay and also makes Doppler Effect non-negligible. The speed of sound in water is expressed as [14]

$$\begin{aligned} v \;=\; & 1448.96 + 4.591\theta - 0.05304\theta^2 + 0.0002374\theta^3 \\ & + 1.340(S-35) + 0.0163z + 1.675\times10^{-7}z^2 \\ & - 0.01025\theta(S-35) - 7.139\times10^{-13}\theta z^3 \end{aligned} \tag{17}$$

where θ is the temperature between 0 and 30^oC, S is the salinity between 30 and 40 parts per million (ppm) and z is the depth between 0 and 8000 m.

C. Ambient Noise

Ambient (colored) noise is usually defined by the Empirical formulas (in dB re μPa per Hz where f is in kHz) [13]:

$$\begin{aligned} 10\log N_{tb}(f) &= 17 - 30\log(f) \\ 10\log N_{s}(f) &= 40 + 20(s-0.5) + 26\log(f) - 60\log(f+0.03) \\ 10\log N_{w}(f) &= 50 + 7.5w^{0.5} + 20\log(f) - 40\log(f+0.4) \\ 10\log N_{th}(f) &= -15 + 20\log(f) \end{aligned} \tag{18}$$

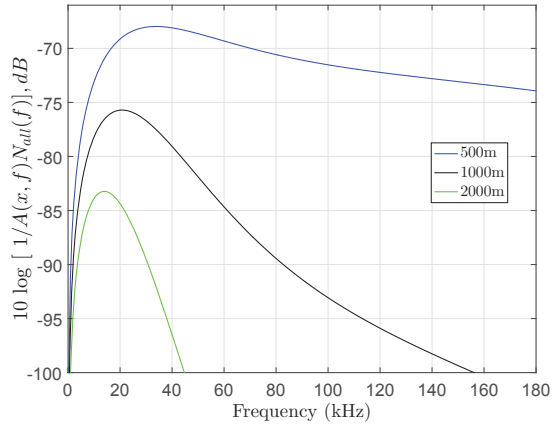

Fig. 4. Optimum operating frequency range for a given transmission distance

where N_{tb} is the turbulence noise, N_s is the shipping noise (s is the shipping factor which takes a value between 0 and 1), N_w is the noise due to breaking waves caused by wind (w represents the speed of wind in m/s) and N_{th} is the thermal noise. The overall power spectral density (PSD) of the ambient noise is expressed as (in μPa) [13]:

$$N_{all}(f) \;=\; N_{tb}(f)+N_s(f)+N_w(f)+N_{th}(f) \tag{19}$$

D. Signal-to-Noise Ratio (SNR)

For a transmitted signal power P, the narrowband SNR is expressed in μPa re dB per Hz as follows [13]

$$SNR(x,f) \;=\; \frac{P/A(x,f)}{N_{all}(f)\Delta(f)}=\frac{S_{tx}(f)}{N_{all}(f)A(x,f)} \tag{20}$$

where $\Delta(f)$ is the bandwidth of the receiver noise and $S_{tx}(f)$ is the PSD of the transmitted signal. As shown in Fig. 4 there exists an optimum frequency for each transmitter-receiver separation at which maximum narrowband SNR is achieved at the receiver.

E. Multipath Propagation

In shallow water horizontal channels, multiple arrivals of the same signal are mainly due to bottom and surface reflections. For the case of deep water, multipath is mainly due to wave refractions because of the spatial variations in acoustic speed [1]. The frequency response of the rth path in a multipath environment is given by [15]

$$H_r(f) \;=\; \Gamma_r/\sqrt{A(x_r,f)}, \tag{21}$$

where x_r is the length of the rth propagation path with a delay of $\tau_r=(x_r/v)-t_0$ (t_0 denotes a reference time at the receiver), Γ_r is the cumulative reflection coefficient for surface and bottom reflections. The overall CFR is given by [15]

$$H(f) \;=\; \sum_r H_r(f)e^{-j2\pi f\tau_r}. \tag{22}$$

The inverse Fast Fourier Transform (IFFT) of (22) results in the following impulse response

$$h(t) \;=\; \sum_r h_r(t-\tau_r). \tag{23}$$

A baseband model of the UAC with discrete multipath components can be represented as follows [13]

$$h(\tau,t) \;=\; \sum_r \Omega_r(t)\delta(\tau-\tau_r(t)), \tag{24}$$

where Ω_r represents the amplitude of the rth propagation path. For a given data block, a Doppler scale factor ξ can be applied to each path delay as follows [13]

$$\tau_r(t)=\tau_r-\xi_r t. \tag{25}$$

For N_{pa} discrete paths, the UAC model can be written as [13]

$$h(\tau,t)=\sum_{r=1}^{N_{pa}}\Omega_r\delta(\tau-[\tau_r-\xi_r t]). \tag{26}$$

IV. Simulation Results

We first consider a horizontally-configured time-varying channel of link distance 1000 m and water depth of 50 m (shallow water). The transmitter and receiver are located at a depth of 48 m and 6 m respectively. The bandwidth of the system is 25 kHz with a carrier frequency f_c of 32.5 kHz. Considering a relative speed of 0.5 m/s between the transmitter and receiver, the maximum Doppler frequency is approximately 11 Hz. A statistical model of the UAC is used where the channel coefficients are obtained using the maximum entropy principle [16]. The Doppler spread is assumed to increase linearly from 0.5 Hz to 2 Hz with the tap delay. The horizontal channel impulse response (CIR) and time-delay response are shown in Fig. 5 where the maximum delay spread is 18.6 ms. The BER performance for the MIMO-OFDM and MIMO-OFDM/OQAM systems in the horizontal UAC is shown in Fig. 6. Colored noise is considered in the simulations to better reflect the real-world underwater noise. The other parameters include 16-QAM modulation and 1024 subcarriers. The CP duration for the OFDM system is 20.48 ms. The preambles for the MIMO-OFDM and MIMO-OFDM/OQAM systems span over 2 complex symbol durations and 5 real symbol durations respectively for N_t=2. For N_t=4, the preamble lengths are 4 complex symbol durations and 9 real symbol durations for the MIMO-OFDM and MIMO-OFDM/OQAM systems respectively. The OFDM/OQAM system is based on a Hermite prototype filter with an overlapping factor of K=4. A single-tap equalizer is used for the MIMO-OFDM system while the receiver structure for the MIMO-OFDM/OQAM system consists of a 3-tap equalizer which is implemented using the frequency-sampling approach [17]. It is to be noted that in FBMC systems, the subcarriers may not necessarily experience flat-fading since the lack of a cyclic prefix implies that the condition for circular convolution is not satisfied. As the channel time dispersion increases, it is desirable to have a large number of subcarriers for them to experience flat-fading and therefore a single-tap equalizer can be used. As can be observed in Fig. 6, the MIMO-OFDM/OQAM systems achieve better performance than the MIMO-OFDM systems in the horizontal UAC for the same transmission time. This shows the robustness of OFDM/OQAM against both time and frequency

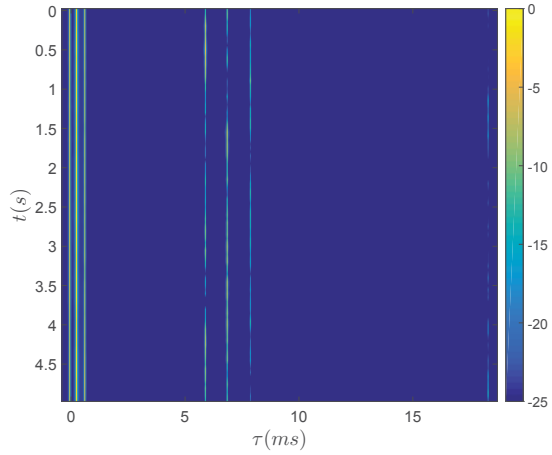

(a)

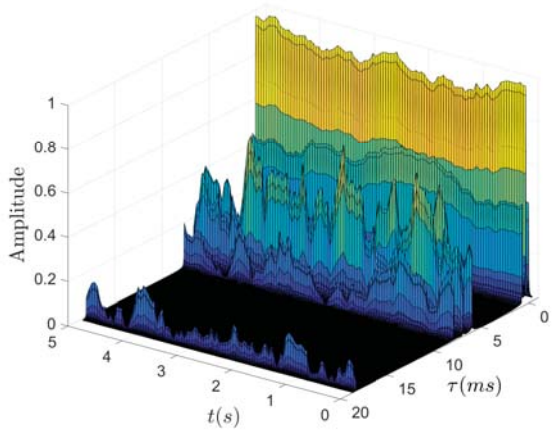

(b)

Fig. 5. Horizontal Channel (a) CIR (b) Time-Delay response

dispersions. When the number of transmitters is increased from 2 to 4, the performance is worse because of cross-talk between parallel channels. In [8], it was stated that the maximum number of transmitters in a MIMO-OFDM system depends on the number of subcarriers and multipath spread of the channel. Considering the 1/2-rate Turbo-coded MIMO systems, at a BER of 10^{-4}, the 2×12 and 4×12 OFDM/OQAM systems yield 4 dB and 8 dB better performance than the 2×12 and 4×12 OFDM systems respectively.

For the vertically-configured channel, the transmitter and receiver are submerged at a depth of 998 m and 1 m respectively. The horizontal separation between them is 1 m. All other parameters are similar to the horizontal channel scenario except for the number of subcarriers and CP duration which are set to 512 and 5.12 ms respectively. The channel responses are shown in Fig. 7 where the delay spread is 3.9 ms. As can be observed in Fig. 8, the MIMO-OFDM/OQAM systems once again outperform the MIMO-OFDM systems. Considering similar transmission time, at a BER of 10^{-4}, the Turbo-coded 2×12 and 4×12 OFDM/OQAM systems outperform the coded OFDM systems with similar MIMO

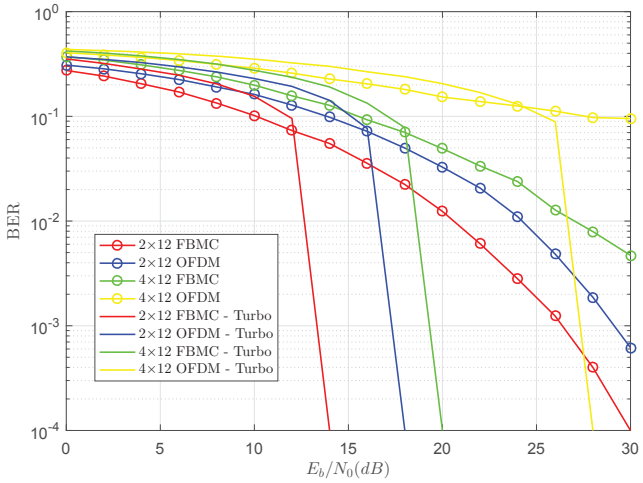

Fig. 6. BER performance of $N_t \times N_r$ OFDM & FBMC in horizontal UAC

TABLE I
THEORETICAL ACHIEVABLE BIT RATE ($kbps$)

Channel Configuration	OFDM		OFDM/OQAM	
	N_t=2	N_t=4	N_t=2	N_t=4
Horizontal	52.6	63.2	73.7	105.3
Vertical	63.2	84.2	73.7	105.3

configuration by 2 dB in both cases.

By taking all overhead due to channel estimation into account and considering similar transmission time for both the OFDM and OFDM/OQAM systems, the theoretical achievable bit rates for the MIMO systems in the 1000 m horizontal and vertical UACs are provided in Table I. The parameters as used for the simulations are considered. In the horizontal channel, the 2×12 and 4×12 OFDM/OQAM systems achieve about 40% and 67% higher bit rate than the 2×12 and 4×12 OFDM systems respectively. As for the vertical channel, the increase in bit rate with OFDM/OQAM compared to OFDM is around 17% and 25% for the 2×12 and 4×12 systems respectively.

V. CONCLUSION

While OFDM performs well in a channel characterized by only time dispersion, it is not the case when there is significant frequency dispersion since its filter is only well localized in time and hence ICI may occur. On the other hand, although OFDM/OQAM represents a challenge in terms of channel estimation and application to MIMO, its prototype filters can be designed to provide robust performance in doubly-dispersive channels. It has been shown that OFDM/OQAM not only provides a better error performance than OFDM but also a higher bit rate due to the absence of a CP. This makes OFDM/OQAM very attractive for real-time underwater wireless video transmission. However, the channel configuration also determines the most optimum parameters that can be used. For instance, we have seen that in a horizontally-configured channel we tend to have a higher error rate than in a vertical channel.

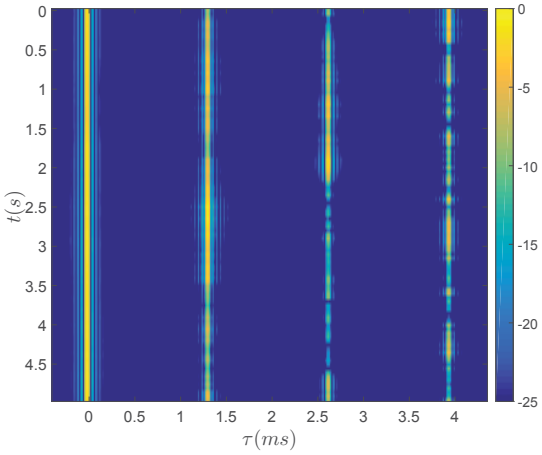

(a)

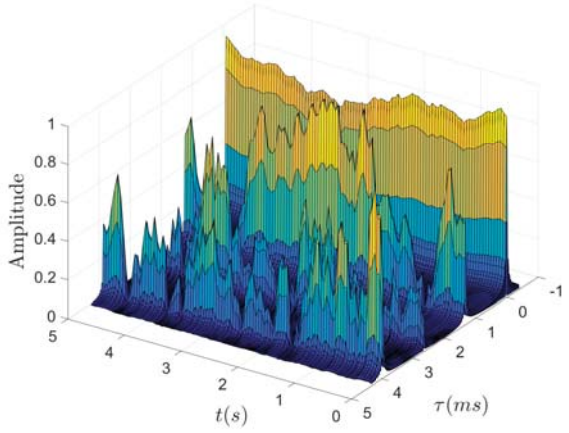

(b)

Fig. 7. Vertical Channel (a) CIR (b) Time-Delay response

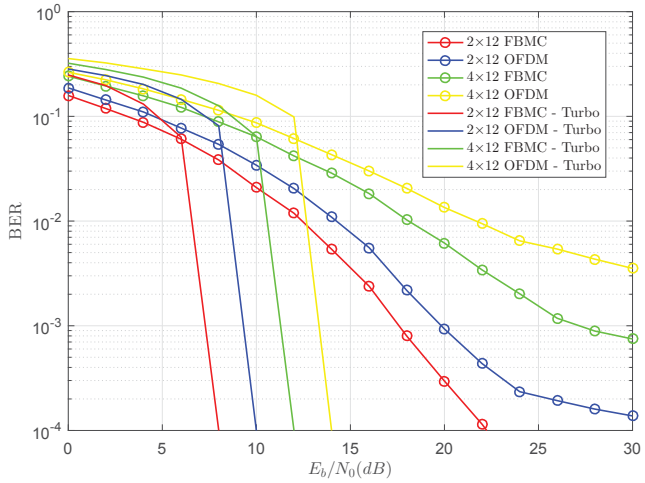

Fig. 8. BER performance of $N_t \times N_r$ OFDM & FBMC in vertical UAC

REFERENCES

[1] M. Stojanovic and J. Preisig, "Underwater acoustic communication channels: Propagation models and statistical characterization," *IEEE Communications Magazine*, vol. 47, no. 1, pp. 84–89, Jan. 2009.

[2] M. Alard, "Construction of a multicarrier signal," Aug. 21 2001, uS Patent 6,278,686.

[3] R. Haas and J.-C. Belfiore, "A time-frequency well-localized pulse for multiple carrier transmission," *Wireless personal communications*, vol. 5, no. 1, pp. 1–18, 1997.

[4] J. Gomes and M. Stojanovic, "Performance analysis of filtered multitone modulation systems for underwater communication," in *OCEANS 2009, MTS/IEEE Biloxi-Marine Technology for Our Future: Global and Local Challenges*. IEEE, 2009, pp. 1–9.

[5] P. Amini *et al.*, "Filterbank multicarrier communications for underwater acoustic channels," *Oceanic Engineering, IEEE Journal of*, vol. 40, no. 1, pp. 115–130, 2015.

[6] A. Aminjavaheri, A. RezazadehReyhani, and B. Farhang-Boroujeny, "Frequency spreading Doppler scaling compensation in underwater acoustic multicarrier communications," in *Communications (ICC), 2015 IEEE International Conference on*, Jun. 2015, pp. 2774–2779.

[7] B. Li *et al.*, "MIMO-OFDM for high-rate underwater acoustic communications," *IEEE Journal of Oceanic Engineering*, vol. 34, no. 4, pp. 634–644, Oct. 2009.

[8] M. Stojanovic, "MIMO OFDM over underwater acoustic channels," in *Proc. Systems and Computers 2009 Conf. Record of the Forty-Third Asilomar Conf. Signals*, Nov. 2009, pp. 605–609.

[9] E. Kofidis and D. Katselis, "Preamble-based channel estimation in MIMO-OFDM/OQAM systems," in *Proc. IEEE Int Signal and Image Processing Applications (ICSIPA) Conf*, Nov. 2011, pp. 579–584.

[10] C. Lélé *et al.*, "Channel estimation methods for preamble-based OFDM/OQAM modulations," *European Transactions on Telecommunications*, vol. 19, pp. 741–750, 2008.

[11] C. Lele, P. Siohan, and R. Legouable, "2 dB better than CP-OFDM with OFDM/OQAM for preamble-based channel estimation," in *Proc. IEEE Int. Conf. Communications*, May 2008, pp. 1302–1306.

[12] J. Du and S. Signell, "Novel preamble-based channel estimation for OFDM/OQAM systems," in *Proc. IEEE Int. Conf. Communications*, Jun. 2009, pp. 1–6.

[13] H. Esmaiel and D. Jiang, "Review article: multicarrier communication for underwater acoustic channel," *Int'l J. of Communications, Network and System Sciences*, vol. 6, no. 08, p. 361, 2013.

[14] M. C. Domingo, "Overview of channel models for underwater wireless communication networks," *Physical Communication*, vol. 1, no. 3, pp. 163–182, 2008.

[15] M. Stojanovic, "Underwater acoustic communications: Design considerations on the physical layer," in *Wireless on Demand Network Systems and Services, 2008. WONS 2008. Fifth Annual Conference on*. IEEE, 2008, pp. 1–10.

[16] F. X. Socheleau *et al.*, "A maximum entropy framework for statistical modeling of underwater acoustic communication channels," in *Proc. OCEANS 2010 IEEE - Sydney*, May 2010, pp. 1–7.

[17] T. Ihalainen *et al.*, "Channel equalization for multi-antenna FBMC/OQAM receivers," *IEEE Transactions on Vehicular Technology*, vol. 60, no. 5, pp. 2070–2085, Jun 2011.